Non-autonomous Vnd acts with autonomous Appl during mushroom body axon growth in *Drosophila*

Claire Marquilly[1], Ana Boulanger[1], Germain U. Busto[1#], Robert P Zinzen[2], Bassem A Hassan[3], Lee G Fradkin[4], and Jean-Maurice Dura[1]

[1] IGH, Univ Montpellier, CNRS, Montpellier, France
[2] Systems Biology Imaging Platform, Max Delbrueck Centrum in der Helmholtz Gemeinschaft, Berlin Institute for Medical Systems Biology, Berlin, Germany
[3] Institut du Cerveau-Paris Brain Institute (ICM), Sorbonne Université, Inserm, CNRS, Hôpital Pitié-Salpêtrière, Paris, France
[4] Institute for Stem Cell Biology and Regenerative Medicine, Stanford University, Stanford, CA USA

[#]Present address: INM, Univ Montpellier, INSERM, Montpellier, France

Abstract

The Amyloid Precursor Protein (APP) is associated with Alzheimer's disease. *Appl* is the single *Drosophila* APP ortholog and is expressed in all neurons throughout development. Appl was previously shown to cell-autonomously modulate axon outgrowth in the mushroom bodies (MBs), the fly olfactory memory center. However, we found that $Appl^{d}$, the only reported null allele, affects the normal function of *vnd*, the gene just proximal to *Appl*. To decipher developmental defects specifically due to a loss of only *Appl* function, we generated a precise *Appl* null allele ($Appl^{C2.1}$) by CRISPR/Cas9 genomic engineering. With $Appl^{C2.1}$, we confirmed the partial requirement for *Appl* in MB axon outgrowth. We also produced new CRISPR *vnd* alleles removing either *vnd-B* or *vnd-A* function. We report here that *vnd* is also required for MB β-branch axon outgrowth and to a much greater extent than *Appl* itself. Moreover, *vnd* is expressed in neurons close to, but not within, the MB during development and is required non-cell-autonomously for MB axon outgrowth

Introduction

Alzheimer's disease (AD) is associated with extracellular accumulation of amyloid fibrils derived from the Amyloid Precursor Protein (APP). APPs have therefore been intensely investigated, however their physiological function in the brain remains unclear and controversial (Nicolas and Hassan, 2014; Selkoe and Hardy, 2016; Soldano and Hassan, 2014). Although there are three paralogues in mammals (APP, APLP1 and APLP2), *Drosophila* encodes a single APP homologue, called *Appl*, that is expressed in all neurons throughout development. It has been shown that the type I transmembrane protein coding gene *Appl* is a conserved neuronal modulator of a Wnt planar cell polarity (Wnt/PCP) pathway, a regulator of cellular orientation within the plane of an epithelium (Soldano et al., 2013). It has been proposed that Appl is part of the membrane complex

formed by the core PCP receptors Fz (*frizzled*) and Vang (*Van Gogh*) required for axon growth (Liu et al., 2021; Soldano et al., 2013).

The mushroom bodies (MBs) are two bilaterally symmetric structures in the central brain that are required for learning and memory (Lin, 2023). Each MB is comprised of 2000 neurons that arise from 4 neuroblasts. Three types of neurons appear sequentially during development: the embryonic/early larval γ, the larval α'β', and the late larval/pupal αβ types. Each αβ neuron projects an axon that branches to send an α branch dorsally, which contributes to the formation of the α lobe, and a β branch medially, which contributes to the formation of the β lobe (Lee et al., 1999). Appl's expression continues in adult flies, notably in the MB αβ neurons (Leyssen et al., 2005; Rabah et al., 2025). So far, *Appl*^{d} is the only reported null *Appl* allele and it results from a synthetic genomic deletion removing the *Appl* locus (Luo et al., 1992). The *Appl*^{d}-bearing chromosome was selected, after γ irradiation, as a translocation of a partial duplication of the X chromosome on the Y chromosome to a X chromosome terminal deficiency (S1 Fig). *Appl*^{d} flies are viable, fertile and display no gross structural defects in the brain (Luo et al., 1992). However, the *Appl* signaling pathway is required for proper axon outgrowth in the MBs since *Appl*^{d} flies display modestly penetrant axonal defects in αβ neurons. Importantly, Appl is required cell-autonomously for β-branch axon outgrowth (Cassar and Kretzschmar, 2016; Soldano et al., 2013).

The *ventral nervous system defective* (*vnd*) gene, which is immediately proximal to *Appl*, encodes a Nk2-class homeodomain transcription factor, that acts in a context-dependent manner as an activator or repressor and is essential for the development of the nervous system. The *vnd* gene encodes two proteins: Vnd-A and Vnd-B whose mRNAs arise from two different promoters. These two proteins differ in their aminoterminal domains and are identical in the remainder of their sequences. While Vnd-A is a transcription repressor for promoters containing Nk-2 binding sites, Vnd-B directly activates transcription, also likely via binding to the same binding site. (Stepchenko et al., 2011). Flies bearing a null allele of vnd in hemi- or homozygous condition are embryonic lethal (Jimenez et al., 1995).

Interestingly, we found that the *Appl*^{d} chromosome also genetically affects *vnd* function. To genetically dissect *Appl* and *vnd* functions, we generated CRISPR alleles that precisely delete the *Appl* gene without affecting *vnd* function (*Appl*$^{C2.1)}$ and that precisely delete each one of the two *vnd* transcripts without affecting *Appl* (*vnd*$^{C\Delta A}$ and *vnd*$^{C\Delta B}$). To analyze the exact developmental defects due to the specific loss of the *Appl* function only, we used *Appl*$^{C2.1}$ and first confirmed the partial requirement of *Appl* in MB β-branch axon outgrowth. We showed here that *vnd-A,* but not *vnd-B,* is also required for MB β-branch axon outgrowth. Unexpectedly, *vnd* is expressed in neurons close to, but not within, the MB during development and is required non-cell-autonomously, likely by promoting the production of a secreted factor(s) involved in the MB axon outgrowth.

Results

Generating new *Appl* CRISPR alleles

The complex chromosome structure resulting in the *Appl*^{d} allele complicates its subsequent genetic manipulation and might be a reason for the sensitivity of its phenotype to genetic background (S1 Fig). Therefore, we produced new null *Appl* alleles by removing the entire *Appl* transcriptional unit via CRISPR/Cas9-mediated deletion (Doudna and Charpentier, 2014). We

recovered *Appl*$^{C1.4}$ and *Appl*$^{C2.1}$, two CRISPR *Appl* null alleles (Fig 1 and S2 Fig), following an adaptation of a published protocol to produce ~50kb deletions (Port et al., 2014). *Appl*^{d} MBs display a modestly penetrant cell-autonomous axon growth defect of the β-branches which manifests as an absence of the β lobe (Liu et al., 2021; Soldano et al., 2013).

Surprisingly, we found a strong difference in the penetrance of the absence of the β lobe phenotype in the two *Appl* CRISPR alleles. Although 9% of *Appl*$^{C2.1}$ MBs lacked the β lobe, slightly lower than the 14.5% described for *Appl*^{d} (Marquilly et al., 2021), *Appl*$^{C1.4}$ MBs displayed a much higher penetrance (66%) of this phenotype (Fig 1). We determined the extents of the precise deletions present in the two alleles via sequencing of PCR amplicons and found that while the *Appl*$^{C2.1}$ deletion precisely removed the *Appl* transcriptional unit, the *Appl*$^{C1.4}$ allele also removed a part of the *vnd* transcriptional unit (Fig 1). We then similarly mapped the *Appl*^{d} deletion and found that, unlike *Appl*$^{C2.1}$, it removes most of the intergenic region between *Appl* and *vnd* which possibly influences *vnd* function (Fig 1). We then assessed, by genetic complementation tests, if the different *Appl* null alleles possibly affected *vnd* function. We used *vnd*^{A}, a molecularly characterized lethal allele which impacts both the *vnd-A* and *vnd-B* transcripts (Fig 2) (Haelterman et al., 2014). Although *Appl*$^{C2.1}$/*vnd*^{A} transheterozygous MBs displayed no anatomical MB phenotypes, the *Appl*^{d}/*vnd*^{A} and *Appl*$^{C1.4}$/*vnd*^{A} MBs displayed 14% and 69% of β lobe absence, respectively (Fig 2). Flies heterozygous for any of the four mutations individually displayed no MB phenotypes: *vnd*^{A}/+ (n = 72), *Appl*$^{C1.4}$/+ (n = 60), *Appl*$^{C2.1}$/+ (n = 42) and *Appl*^{d}/+ previously described (Soldano et al., 2013). Therefore, *Appl*^{d} and *Appl*$^{C1.4}$, but not *Appl*$^{C2.1}$ affect *vnd* functions in MB development. We could write *Appl*^{d} = *Appl*^{null} *vnd*^{weak}, *Appl*$^{C1.4}$ = *Appl*^{null} *vnd*^{strong} and only *Appl*$^{C2.1}$ = *Appl*^{null} *vnd*$^{+}$. Taken together, these data strongly suggest that *vnd* is also involved in the MB β-branch axon growth and likely to a much greater extent than *Appl* itself.

Generation of new *vnd* CRISPR alleles deleted either for *vnd-B* or *vnd-A* function.

The two *vnd* transcripts, *vnd-A* and *vnd-B*, produce two different Vnd proteins, respectively Vnd-A and Vnd-B (Fig 2). It was proposed that, while Vnd-A has its main role during embryogenesis, Vnd-B acts during metamorphosis (Stepchenko et al., 2011). To determine which Vnd isoform is required for MB β-branch axon growth, we produced the new *vnd* alleles *vnd*$^{C\Delta A}$ and *vnd*$^{C\Delta B}$ by CRISPR/Cas9 genomic engineering that eliminate either the *vnd-A* or the *vnd-B* isoform, respectively (Fig 3 and S3 Fig). Males bearing a *vnd*$^{C\Delta B}$ mutant allele (*vnd*$^{C\Delta B}$/Y), as well as *vnd*$^{C\Delta B}$/ *Appl*$^{C1.4}$ females, are viable and have essentially wild-type MBs (Fig 3). Males bearing a *vnd*$^{C\Delta A}$ mutant allele (*vnd*$^{C\Delta A}$/Y) are embryonic lethal similarly to other *vnd* null alleles which affect both isoforms. *Appl*$^{C1.4}$/*vnd*$^{C\Delta A}$ female MBs displayed a strong phenotype of β lobe absence with a penetrance (64%) like those of *Appl*$^{C1.4}$/*vnd*^{A} female MBs (Fig 4). We sought to determine the respective contribution of the lack of *Appl*$^{+}$ and the lack of *vnd*$^{+}$ for the strong β lobe absence in *Appl*$^{C1.4}$/*vnd*$^{C\Delta A}$ females. For this purpose, we added either a duplication of *Appl*$^{+}$ or a duplication of *vnd*$^{+}$ to this genotype. We found that *Appl*$^{C1.4}$/*vnd*$^{C\Delta A}$; *Dp-Appl*$^{+}$/+ females displayed 69% of β lobe absence, a penetrance not distinguishable from that observed without the duplication of wildtype *Appl* (p = 0.42). Therefore, in these two types of females (*Appl*$^{C1.4}$/*vnd*$^{C\Delta A}$; +/+ *and* *Appl*$^{C1.4}$/*vnd*$^{C\Delta A}$; *Dp-Appl*$^{+}$/+), the phenotype of β lobe absence seemed entirely due only to *vnd* lack-of-function. Indeed, *Appl*$^{C1.4}$/*vnd*$^{C\Delta A}$; +/+ females could be considered as *Appl*^{null} *vnd*^{strong}/*Appl*$^{+}$ *vnd*^{null} being homozygous mutant for *vnd* but heterozygous null for *Appl*. Similarly, *Appl*$^{C1.4}$/*vnd*$^{C\Delta A}$; *Dp-Appl*$^{+}$/+ females could be considered as *Appl*^{null} *vnd*^{strong}/*Appl*$^{+}$ *vnd*^{null}; *Dp-*

Appl^{+}/+ and are homozygous mutant for *vnd* but wild-type for *Appl*. Supporting the hypothesis of Vnd role in β axon growth, we observed a complete rescue when an extra dose of *vnd*$^{+}$ is supplied as in *Appl*$^{C1.4}$/*vnd*$^{C\Delta A}$; *Dp-vnd*$^{+}$/+ females (Fig 4). *Appl*$^{C1.4}$/Y males have no *Appl*$^{+}$ function (null allele) and display reduced *vnd*$^{+}$ function. Moreover, *Appl*$^{C1.4}$/Y male MB phenotype is moderately rescued by the presence of an extra dose of *Appl*$^{+}$ but strongly rescued by an extra dose of *vnd*$^{+}$ (Fig 4). Taken together, these results strongly indicate that the *vnd-A* transcript but not the *vnd-B* transcript is specifically required for MB β-branch axon growth.

Vnd is expressed around the MBs and is not required within the MBs.

In order to know where *vnd* is expressed, we employed a *vnd-T2A-GAL4* line where GAL4 is under the control of endogenous *vnd* regulatory sequences via CRISPR gene targeting so that GAL4 and *vnd* are translated from a single mRNA transcript (Chen et al., 2015; Lee et al., 2020). UAS-GFP labelling revealed a pattern in the ventral ganglion of the third larval instar central nervous system (L3 CNS) similar to that described with immunostaining with antibodies against Vnd (Stepchenko et al., 2011) thus validating the use of the *vnd-T2A-GAL4* line as a *bona fide vnd* reporter (S4 Fig). GFP was detected, in the developing brain, close to the MBs visualized by anti-Fas2 staining, from L3 to 24 h after puparium formation (APF) (Fig 5A, A'- 5D, D'). Staining reveals a structure in the brain whose cell bodies are organized in a honeycomb pattern. To determine the identity of the cell bodies, we performed DAPI staining at the L3 stage. We observed a significant DAPI staining in these structures indicating that they correspond to cell nuclei (Fig 5E, E'). Moreover, these cell nuclei are Vnd positive and Repo negative (Fig 5F, F'-5G, G') indicating that these cells correspond to neurons, rather than glia. The neurites emanating from these cell nuclei are very close to the developing MB medial lobe from which the adult β lobe develops (Fig 5). Noticeably, we did not observe any GFP labeling within the MBs themselves. This unexpected expression pattern suggests a non-cell-autonomous role for Vnd in the MB β-branch axon growth. We tested this hypothesis by MARCM mosaic analysis which allowed the generation of homozygous *vnd* loss-of-function MB clones in an otherwise heterozygous genetic background and overcame the homozygous lethality phenotype (Lee et al., 1999; Lee and Luo, 1999). Mitotic recombination was induced in late-stage embryos/early first instar larvae and the clones were analyzed at the adult stage. We obtained 20 MB *vnd*$^{A/A}$ clones that include the αβ neurons. All the 20 *vnd* mutant clones displayed a β-branch axon growth that looked identical to that in wild-type clones (S5 Fig). Moreover, we obtained similar results, namely a normal β-branch axon growth, with two additional different null alleles, *vnd*$^{\Delta 38}$ (8 clones) and *vnd*^{6} (4 clones) (S5 Fig). Taken together, these results demonstrate that, although *vnd* function is strongly required for MB β-branch axon growth, *vnd* is neither required nor expressed in the MBs themselves. Therefore, it is most likely that Vnd regulates MB axon growth by a non-cell-autonomous mechanism.

Discussion

It has been proposed that Appl is part of the membrane complex formed by the core PCP proteins Fz and Vang (Soldano et al., 2013). *Appl*^{d} was, before this report, the only *Appl* null allele described. *Appl*^{d} mutant flies are completely lacking Appl function and exhibit 14.5 % MB β-lobe loss (Marquilly et al., 2021) in accordance with what has been reported (Liu et al., 2021; Soldano

et al., 2013). This modestly penetrant axonal phenotype due to the lack of Appl could be due to partially redundant function provided by the other transmembrane receptors of the complex. Flies homozygous for the loss of function allele *Vang*$^{stbm-6}$ exhibit 50% β-lobe loss (Liu et al., 2021). As the *Appl*^{d} allele involves complex chromosomic rearrangements (Luo et al., 1992), we leveraged CRISPR/Cas9 chromosomal engineering to produce a defined deletion of around 50 kb to specifically eliminate the *Appl* transcriptional unit. We recovered two *Appl* complete deletions (Fig 1): *Appl*$^{C1.4}$ and *Appl*$^{C2.1}$ removing around 52 kb and 47 kb and exhibiting 66 % and 9 % β-lobe loss respectively. DNA sequences analysis revealed that, while the *Appl*$^{C2.1}$ deletion removes only *Appl* sequences, the *Appl*$^{C1.4}$ deletion additionally removes a part of the proximally located transcriptional unit corresponding to the *vnd* gene (Fig 1). This indicates that in addition to Appl, *vnd* is likely involved in the β-branch axon outgrowth. Moreover, as can be expected from the extent of the deletions and based on genetic complementation tests, the *Appl*$^{C1.4}$ deletion, but not the *Appl*$^{C2.1}$ deletion, affects *vnd* function. Most importantly, the *Appl*^{d} deletion, which removes most of the Appl coding sequence and the intergenic region between *Appl* and *vnd*, also affects *vnd* function (Fig 1 and 2).

The role of *vnd* in β-branch axon outgrowth is complicated by the fact that the viable *vnd* mutant alleles (*Appl*^{d} *and* the *Appl*$^{C1.4}$ deletion), do not encode functional Appl. Nevertheless, employing a small (less than 100 kb) genomic *Appl*$^{+}$ duplication, we found that flies lacking only *vnd* function still exhibit 69% β-lobe loss and that this mutant phenotype is completely rescued by a small genomic *vnd*$^{+}$ duplication (Fig 4). This demonstrates a requirement of *vnd* function in MB β-branch axon outgrowth. To better understand the roles of both Vnd isoforms in the MB β-branch axon outgrowth, we produced two mutations, *vnd*$^{C\Delta B}$ and *vnd*$^{C\Delta A}$, which remove the *vnd-B* and the *vnd-A* transcript respectively (Fig 3 and S3 Fig). *vnd-A* mRNA is expressed strongly in embryos and much less in larvae and adults contrarily to *vnd-B* mRNA (Stepchenko et al., 2011). It was therefore expected that the phenotype seen in adult MBs of pupal-born neurons should be due to *vnd-B* rather than *vnd-A*. Surprisingly, although Vnd-A has a significant role in MB axon growth, apparently Vnd-B plays very little to no role in this process. Noticeably, the MB phenotype of *Appl*$^{C1.4}$/*vnd*$^{C\Delta A}$ flies is similar in penetrance to that of *Appl*$^{C1.4}$/*vnd*^{A} where *vnd*^{A} impacts both the *vnd-A* and *vnd-B* transcripts. This indicates that a lack of *vnd-A* function, and not that of vnd-B, underlies the poor β-branch axon outgrowth phenotype.

If Vnd interacts with Appl within the MBs, we hypothesized that it might be expressed within the MBs, and act cell-autonomously like Appl. However, endogenous *vnd* transcription monitored by GAL4 expression that is translated from the same mRNA transcript and was validated by anti-Vnd staining did not reveal Vnd expression within the MBs. Rather, *vnd* is transcribed in cells within a neuronal brain structure near the developing MB medial lobe from which the adult β lobe develops (Fig 5). Using MARCM mosaic analysis, we show that β axons extended from MB clones null for *vnd* function exhibit wild-type growth patterns (S5 Fig) demonstrating a non-cell-autonomous requirement for Vnd. Therefore, we favor the hypothesis that *vnd* expressed in a MB surrounding brain structure causes the expression of one or more secreted factors regulating the axon growth of the developing β medial lobe.

Materials and methods

217 ***Drosophila* stocks**
218 All crosses were performed on standard culture medium at 25˚C. Except where otherwise stated,
219 all alleles and transgenes have been described previously (http://flystocks.bio.indiana.edu/). The
220 following alleles were used: *Appl*$^{C1.4}$, *Appl*$^{C2.1}$, *vnd*$^{C\Delta A}$ and *vnd*$^{C\Delta B}$ were generated in this study. *Appl-*
221 *y*$^{+}$ (BL #56073), *Appl*^{d} (BL #43632), *vnd*^{A} (BL #57139), *vnd*$^{\Delta 38}$ (Chu et al., 1998), *vnd*^{6} (Jimenez et
222 al., 1995). The following transgenes were used: *UAS-mCD8::GFP* (BL #5137) and the duplications
223 resulting from genomic transgenes *Dp(1;3) DC430* (BL #32288) and *Dp(1.3) DC009* (BL #30219)
224 which are both inserted into the same attP site at 65B2. For simplicity, we refer to *Dp(1;3) DC430*
225 as *Dp-Appl*$^{+}$ and *Dp(1.3) DC009* as *Dp-vnd*$^{+}$. *Dp-Appl*$^{+}$ is ~ 97 kb and contains 11 genes including
226 the *Appl* gene but not the *vnd* gene. *Dp-vnd*$^{+}$ is also ~ 97 kb and contains 15 genes including the
227 *vnd* gene but not the *Appl* gene. We used two GAL4 lines: *vnd-T2A-GAL4* (Lee et al., 2020) which
228 reveals *vnd* transcription and *c739-GAL4* (BL #7362) expressed in adult αβ MB neurons (Aso et al.,
229 2009). Recombinant chromosomes were obtained by standard genetic procedures. In the case of
230 the recombination between *y*$^{+}$ and *ApplC*$^{2.1}$ (~ 170 kb apart) we screened for [*y*$^{+}$] viable males
231 coming from *y*$^{+}$ *vnd*$^{\Delta 38}$/*y ApplC*$^{2.1}$ females. Note that *vnd*$^{\Delta 38}$ is an embryonic lethal mutation. Four
232 [*y*$^{+}$] viable males out of 11320 males were obtained. One male was sterile, but three *y*$^{+}$ *ApplC*$^{2.1}$ /Y
233 males gave progeny (percentage of recombination circa 0.027%) and were confirmed by genomic
234 PCR. MARCM stocks: *tubP-GAL80, hsFLP122, hsFLP1, FRT19A* (all on the X chromosome).
235
236 **CRISPR-Cas9 strategy**
237 All guide RNA sequences (single guide RNA (sgRNA)) were selected using the algorithm
238 targetfinder.flycrispr.neuro.brown.edu/ containing 20 nucleotides each (PAM excluded) and are
239 predicted to have zero off-targets. We selected one pair of sgRNA for the *Appl* gene and two pairs
240 of sgRNA for the *vnd* gene. For *Appl*, the pair is targeting the entire transcriptional unit (S2 Fig).
241 For *vnd*, each pair is targeting either the A specific region of *vnd* or the B specific region of *vnd* (S3
242 Fig). We used the following oligonucleotide pairs: CRISPR-1 Appl fwd and CRISPR-1 Appl rev to
243 target the all *Appl* region, CRISPR-1 vnd A fwd and CRISPR-1 vnd A rev to target the A region of
244 *vnd*, CRISPR-1 vnd B fwd and CRISPR-1 vnd B rev to target the B region of *vnd* (see the
245 corresponding oligonucleotide sequences in S2 and S3 Fig.). We introduced two sgRNA sequences
246 into pCFD4 (Port et al., 2014), a gift from Simon Bullock (Addgene plasmid # 49411) by Gibson
247 Assembly (New England Biolabs) following the detailed protocol at crisprflydesign.org. For PCR
248 amplification, we used the protocol described on that website. Construct injection was performed
249 by Bestgene (Chino Hills, CA) and all the transgenes were inserted into the same attP site
250 (VK00027 at 89E11). Being aware that the DNA excision of nearly 50 kb might be rare, we have
251 decided to use a positive screen before validation by genomic PCR. We have used a stock where
252 the *Appl* gene is marked by a *y*$^{+}$ construct. The deletion of the *Appl* gene should therefore be
253 associated to *y*$^{-}$ phenotype. Transgenic males expressing the *Appl* sgRNAs and bearing an
254 isogenized X chromosome (*y Appl-y*$^{+}$ *Act-Cas9 w**) were crossed to *FM7c/ph*^{0} *w* females. 180
255 crosses were set up and only two crosses gave rise to *y Appl*$^{deletion?}$ *Act-Cas9 w*/FM7c* females
256 indicating 1% of CRISPR efficacy. From each of these two crosses, a single *y Appl*^{deletion} *Act-Cas9*
257 *w* /FM7c* female was crossed with *FM7c* males to make a stock (*Appl*$^{C1.4}$ and *Appl*$^{C2.1}$ where Cas9
258 was removed). The deletion was then validated by genomic PCR using two pairs of primers:
259 *Appl*$^{C1.4}$ fwd (GAGCCAGATACACAAGCACA) / *Appl*$^{C1.4}$ rev (GGCTTTGTTTACTTCCTGGC) and *Appl*$^{C2.1}$
260 fwd (TCCTACTACGTTCCACAATC) / *Appl*$^{C2.1}$ rev (TAATGCCCAACATATCCAAC). The precise

261 endpoints of the deletion were determined by sequencing (Genewiz, France). Transgenic males
262 expressing the different *vnd* sgRNAs were crossed to *y nos-Cas9 w** females bearing an isogenized
263 X chromosome. 100 crosses were set up for each sgRNA pair, with up to 5 males (because of poor
264 viability) containing both the sgRNAs and *nos-Cas9,* and 5 *FM7c/ph^{0} w* females. From each
265 selected cross, a single *y vnd$^{deletion?}$ nos-Cas9 w* /FM7c* female was crossed with *FM7c* males to
266 make a stock which was validated for the presence of an indel by genomic PCR with primers
267 flanking the anticipated deletion and the precise endpoints of the deletion were determined by
268 sequencing (Genewiz, France) using *vnd*-specific primers: *vnd$^{C\Delta A}$* fwd (ccaacaaagccgagagtctct) /
269 *vnd$^{C\Delta A}$* rev (cgggaatttctaagccagggt) and *vnd$^{C\Delta B}$* fwd (cgatttggggcgttgtgagta) / *vnd$^{C\Delta B}$* rev
270 (gttgggctttaatccgggagt). A CRISPR efficacy of at least 5% was obtained in both cases. We kept a
271 single stock from each set of CRISPR experiment: *vnd$^{C\Delta A}$* and *vnd$^{C\Delta B}$* where Cas9 was removed.
272
273 **Brain dissection, immunostaining and MARCM mosaic analysis**
274 Adult fly heads and thoraxes were fixed for 1 h in 3.7% formaldehyde in phosphate-buffered
275 saline (PBS) and brains were dissected in PBS. For larval and pupal brains, brains were first
276 dissected in PBS and then fixed for 15 min in 3.7% formaldehyde in PBS. They were then treated
277 for immunostaining as described (Boulanger et al., 2011; Lee and Luo, 1999). Antibodies, obtained
278 from the Developmental Studies Hybridoma Bank, were used at the following dilutions: Mouse
279 monoclonal anti–Fas2 (1D4) 1:10, mouse monoclonal anti-Repo (8D1.2) 1:10 and guinea pig
280 polyclonal anti-vnd (1/1000). Goat secondary antibodies conjugated to Cy3 against mouse or
281 guinea pig IgG (Jackson Immunoresearch laboratory) were used at 1:300 for detection. DAPI
282 (Sigma) was used after secondary antibody washes. Tissues were incubated for 10 minutes at
283 room temperature in a 1/1000 solution from a stock containing 1 mg/ml of DAPI solution, then
284 washed. To generate clones in the MB, we used the MARCM technique (Lee and Luo, 1999). First
285 instar larvae were heat-shocked at 37°C for 1 h. Adult brains were fixed for 15 min in 3,7%
286 formaldehyde in PBS before dissection and GFP visualization.
287
288 **Production of the anti-Vnd antiserum**
289 Full length vnd-RA was amplified via PCR from cDNA and cloned into a pRSET bacterial expression
290 vector (ThermoFisher) in frame with an N-terminal 6x-His tag, amplified in DH5alpha and
291 transformed into BL21 competent cells for protein production. His-tagged VndA was purified over
292 a Nickel-NTA agarose resin (Qiagen) according to manufacturer's recommendation. Purified
293 protein was injected into guinea pigs by Squarix GmbH (Marl, Germany, www.squarix.de),
294 selected by determining that pre-immunization sera did not produce signal in Western blots of
295 fly extracts. Successive bleeds were screened for distinct signal in Western blots using embryo
296 extracts and by immunohistochemistry, where signal was expected post 2.5hrs AED.
297
298 **Microscopy and image processing**
299 Images were acquired at room temperature using a Zeiss LSM 780) equipped with a 40x PLAN
300 apochromatic 1.3 oil-immersion differential interference contrast objective lens and a Leica SP8
301 laser scanning confocal microscopes (MRI Platform, Institute of Human Genetics, Montpellier,
302 France. The immersion medium used was Immersol 518F. The acquisition software used was Zen
303 2011 (black edition) for the Zeiss and LasX for the Leica. Contrast and relative intensities of the

green (GFP), of the red (Cy3) and of the DAPI channels were processed with ImageJ (Fiji) software. Settings were optimized for detection without saturating the signal.

Statistics

Comparison between two groups expressing a qualitative variable was analyzed for statistical significance using the Chi^2 test. (BiostaTGV: http://biostatgv.sentiweb.fr/?module=tests). Values of $p < 0.05$ were considered to be significant. Statistical significance was defined as: ns = not statistically different, **p<0.01 and****p<0.0001.

Figure legends

Fig 1. Generating new *Appl* CRISPR alleles.

(A) Schematic representation of *Appl* (blue) and *vnd* (green) genes and transcripts. White boxes represent 5'UTR and 3'UTR, blue and green boxes represent *Appl* and *vnd* coding sequences respectively. Schematic representations of the $Appl^{d}$, $Appl^{C1.4}$ and $Appl^{C2.1}$ mutant alleles where the deleted sequences are represented in light blue. The hatched black segment represents the uncertainty where the deletion of $Appl^{d}$ starts at its 5'end. (B) Representation of the 3' limit of the $Appl^{d}$, $Appl^{C1.4}$ and $Appl^{C2.1}$ mutant alleles (light blue). The hatched black segment represents the uncertainty where the $Appl^{d}$ deletion ends in 3'. The orange star represents the position of the 3' sgRNA used to create the two CRISPR deletions. (C) Wild-type (WT) MB revealed by an anti-Fas2 staining. The pink and yellow arrowheads show respectively the α and β lobe (n=216 MBs). (D-E) Anti-Fas2 staining reveals the loss of β lobe on a representative $Appl^{C1.4}$ brain (n=147 MBs) (D) and on $Appl^{C2.1}$ brain (n=253 MBs) (E). The % represents the proportion of loss of β lobe for each genotype. Scale bar = 50 µm. Full genotypes: (C) Canton-S. (D) y $Appl^{C1.4}$ w^{1118}/Y. (E) $Appl^{C2.1}$/Y.

Fig 2. $Appl^{d}$ and $Appl^{C1.4}$, but not $Appl^{C2.1}$, are impaired for *vnd* function.

A) Schematic representation of *vnd* gene and transcripts. White boxes represent 5'UTR and 3'UTR, green boxes represent coding sequences. Red star represents point mutation on vnd^{A} allele. Schematic representation of *vnd-B* and *vnd-A* transcripts. The vnd^{A} mutation affects both transcripts. (B-D) Anti-Fas2 staining reveals the loss of β lobe on a representative $Appl^{d}$/ vnd^{A} brain (n=214 MBs) (B), $Appl^{C1.4}$/ vnd^{A} brain (n=147 MB) (C) but not on $Appl^{C2.1}$/ vnd^{A} brain (n=248 MBs) (D). The % represents the proportion of loss of β lobe for each genotype. Scale bar = 50 µm. Full genotypes: (B) $Appl^{d}$/y vnd^{A} *w* FRT19A*. (C) y $Appl^{C1.4}$ w^{1118}/ y vnd^{A} *w* FRT19A*. (D) $Appl^{C2.1}$/ y vnd^{A} *w* FRT19A*.

Fig 3. Generating new *vnd* CRISPR alleles deleted either for the *vnd-B* or the *vnd-A* function.

(A) Schematic representation of *vnd* gene and transcripts. White boxes represent 5'UTR and 3'UTR, green boxes represent coding sequences. The deleted sequence region of $vnd^{C\Delta A}$ and $vnd^{C\Delta B}$ are represented in light green. (B-C) Anti- Fas2 staining reveals essentially wild-type looking MBs on a representative $vnd^{C\Delta B}$ brain (n=146 MBs) (B) and $Appl^{C1.4}$/ $vnd^{C\Delta B}$ brain (n=159 MB) (C). The % represents the proportion of loss of β lobe for each genotype. Scale bar = 50 µm. Full genotypes: (B) *y* $vnd^{C\Delta B}$ w^{1118}/Y. (C) y $Appl^{C1.4}$ w^{1118}/ *y* $vnd^{C\Delta B}$ w^{1118}

348 **Fig 4. Vnd-A is required for MB β-branch axon outgrowth.**
349 (A) Quantitation of the rescue of MB β lobe absence of *Appl*$^{C1.4}$/Y (66%; n= 147 MBs, see a
350 representative brain in Fig.1D) and *Appl*$^{C1.4}$/*vnd*$^{C\Delta A}$ (64%; n=198 MBs) (light blue) by an *Appl*
351 duplication (dark blue) (50%; n=150 MBs, 69%; n=89 MBs) and by a *vnd* duplication (green) (3%;
352 n=191 MBs ; 0%; n=164 MBs). **p<0.01 and ****p<0.0001. (B-D) Anti-Fas2 staining on a
353 representative rescued *Appl*$^{C1.4}$/Y; *Dp-vnd*$^{+}$/+ brain (B), *Appl*$^{C1.4}$/*vnd*$^{C\Delta A}$; +/+ brain (C) and on
354 *Appl*$^{C1.4}$/*vnd*$^{C\Delta A}$; *Dp-vnd*$^{+}$/+ brain (D). The % represents the proportion of loss of β lobe for each
355 genotype. Scale bar = 50 µm. Full genotypes: (B) y *Appl*$^{C1.4}$ *w*^{1118}/Y; *Dp-vnd*$^{+}$/+. (C) y *Appl*$^{C1.4}$ *w*^{1118}/*y*
356 *vnd*$^{C\Delta A}$ *w*^{1118}; +/+. (D) y *Appl*$^{C1.4}$ *w*^{1118}/*y vnd*$^{C\Delta A}$ *w*^{1118}; *Dp-vnd*$^{+}$/+.
357
358 **Fig 5. *vnd* is expressed close to the developing MB medial lobe.**
359 (A-D) Visualization of *vnd* expression in brain using *vnd-GAL4* driven *UAS-GFP* at L3, 0h, 6h, and
360 24h APF. GFP was visualized on green and anti-FasII staining labelling of MB axons on red. A-D are
361 confocal z stacks taken the whole MB and A'-D' are stacks of five sections from A-D respectively
362 comprising GFP^{+} regions surrounding MB. Arrowheads point to *vnd-GAL4* driven *UAS-GFP*
363 neurites that surround MB medial lobes, which correspond to γ lobes from L3 to 6 h APF (A'-C')
364 and β lobes at 24 h APF (D'). n ≥ 10 for each time point. (E-G) show single confocal sections
365 showing *vnd* expression using *vnd-GAL4* driven *UAS-GFP* (single channel) at L3. E' to G' are merges
366 of single channel E to G respectively and DAPI staining (red on E'), anti-vnd (red on F') and anti-
367 Repo (red on G'). DAPI labelled nuclei in GFP^{+} cell bodies are pointed by arrows in E'. These nuclei
368 were also Vnd positive (arrows in F') but were not labelled by an anti-Repo (white arrow in G')
369 which labels glia nuclei (red dots pointed by a yellow arrow in G') indicating that these Vnd
370 positive nuclei belong to neurons. Scale bars are 50 µm. n ≥ 5 brains for each type of staining.
371 Full genotype: *vnd-T2A-GAL4 w**; 2 x *UAS-mGFP*/+.
372
373
374 ## Supporting information
375
376 **S1 Fig. Scheme of *Appl*^{d} chromosomic organization**
377 (A) Schematic representation of *Appl*^{d} mutant allele. The upper panel represents the wild-type
378 (WT) X (black) and Y (orange) chromosomes. The *elav*, *Appl* and *vnd* genes are represented
379 respectively in yellow, blue, and green boxes. The middle panel represents the deficiency Df (1)
380 RT518 on the X chromosome deleting the distal part of the chromosome including the *elav* and
381 *Appl* genes. The X Dup Y chromosome represents a duplication of the X chromosome linked to
382 the Y chromosome including the distal part of the X chromosome including the *elav* gene. The
383 lower panel represents a proposed structure of the *Appl*^{d} chromosome where the deficiency-
384 bearing X chromosome had been linked by gamma irradiation to the X Dup Y chromosome
385 (adapted from (Luo et al., 1992)). Additionally, we found that the Y chromosome behaves
386 genetically as linked to the X chromosome.
387
388 **S2 Fig. Structure of the *Appl*$^{C1.4}$ and *Appl*$^{C2.1}$ CRISPR alleles**
389 (A) Schematic representation of *Appl* (blue) and *vnd* (green) genes and transcripts. White boxes
390 represent 5'UTR and 3'UTR, blue and green boxes represent *Appl* and *vnd* coding sequences

respectively. The yellow stars in *Appl* 5' region and the orange star in *Appl* 3' region represent the position of the sgRNA used to create $Appl^{C1.4}$ and $Appl^{C2.1}$ mutants. The red and blue boxes represent respectively the regions magnified in B and C. (B) Representation of the 5' sequence targeted by the sgRNA (yellow) and the PAM domain (magenta) in the WT chromosome *Appl* (blue) (upper line). The lower line is the sequence of the $Appl^{C1.4}$ mutant showing the beginning of the deletion about 1kb after the region targeted by the sgRNA. (C) Representation of the 3' sequence targeted by the sgRNA (orange) and the PAM domain (magenta) in the WT chromosome *Appl* (blue) and *vnd* (green) (upper line). The lower line is the sequence of the $Appl^{C1.4}$ mutant showing the end of the deletion about 6kb after the region targeted by the sgRNA. (D) Representation of the 5' and 3' sequences targeted by the sgRNA (yellow in 5' and orange in 3') and the PAM domain (magenta) in the WT chromosome *Appl* (blue) (upper line). The lower line is the sequence of the $Appl^{C2.1}$ mutant showing the beginning of the deletion in the sequence targeted by the 5' sgRNA (yellow) and the end of the deletion in the sequence targeted by the 3' sgRNA (orange). Circa 46 kb of *Appl* transcribed sequence including all the coding sequence has been entirely deleted and replaced by a sequence of 821bp (see below) primarily derived from the fly retrotransposon micropia-like LTR polyprotein gene (NCBI Blast)**.**

ATAAACGCGTCATTAAGCTGTTCCATTTTCTAATCGCGCAGCGAGTTTCGGTGGTCGAAGTCTAGAATTGAAAAAGAAGAAGAA
GAAGATACTCTGTATGTTATGGTTAAGAATAAAAGCTTAAGTTCAGTTTGTGTTATGAAACACAAAATGTGCCTTTGAACTTGAT
ATTGGTCATTACACGAGGATGTGTAAATGTCAGATGGTTATCCGTCTATGAGAGACGATGGTTATCCGTCTATGAGAGACGATG
GTTATCCGTCTATGAGAGACGATGGTTATCCGTCCATGAGAGACGATGGTTATCCGTCTATGAGAGACGATGGTTATCCGTCTA
TGAGAGACGATGGTTATCCACCTAAGACAGACGATGATTTCAGTTTAGAATCTCTTGTTACGTAAGAAATTTGAATCAAAATTG
GGAGTACTACACGAGGACGTGTCAAGGTCAGGATGGCCGTGTCGGAGCATACTGTATGTACGCTCTGTATGTGATTGTTGCTG
CGTATTGCACGTACGCGCTGTGTGTGTATTGCTGTGCATGGGAAATCTGGTTTTTACCAGAATTCCTAATTTCATCATATTAGTA
ATATTGCATCAGCCGTTAATTGCGCTCTGATTGGTCCTTTGCATTTTGTCGCTTTAAGAAGTACCGTTTTAGCGAGACGACAGCG
CTACAACGCTGTCGTCGTGTGTGGTTCGGGAGCTATGCGGGGAAGTAAGTCTGGCGTTGTCACGCAGTTTTTATAGAAACGTG
AAAGCATAAGGCACCGAAACTCGCTTCGCTAGGTACGCATATGGCACAAAATAATCAAGTTCTA

S3 Fig. Structure of the $vnd^{C\Delta B}$ and $vnd^{C\Delta A}$ CRISPR alleles

(A) Schematic representation of *vnd* (green) gene and transcripts. White boxes represent 5'UTR and 3'UTR, green boxes represent *vnd* coding sequences. The yellow stars represent the position of the sgRNA used to create $vnd^{C\Delta B}$ mutant. The orange stars represent the position of the sgRNA used to create $vnd^{C\Delta A}$ mutant. (B) Representation of the sequences targeted by the sgRNA (yellow) and the PAM domain (blue) in the WT chromosome *vnd* (green) (upper line). The lower line is the sequence of the $vnd^{C\Delta B}$ mutant showing the beginning of the deletion in the sequence targeted by the 5' sgRNA (yellow) and the end of the deletion in the sequence targeted by the 3' sgRNA (yellow). (C) Representation of the sequences targeted by the sgRNA (orange) and the PAM domain (blue) in the WT chromosome *vnd* (green) (upper line). The lower line is the sequence of the $vnd^{C\Delta A}$ mutant showing the beginning of the deletion at one nucleotide from the sequence targeted by the 5' sgRNA (orange) and the end of the deletion within in the sequence targeted by the 3' sgRNA (orange).

S4 Fig. Vnd L3 CNS labelling

(A-C) Visualization of *vnd* expression in VNC using both *vnd-GAL4* driven *UAS-GFP* (green) and an anti-vnd antibody (red) at L3 stages. Images A-C and A'-C' are the same confocal z-projection.

436 Laser intensities leading to the green color were increased from B, C to B', C' to illustrate the high
437 degree of colocalization between the two markers. Low laser intensity allowed us to show red
438 nuclear vnd staining in only some GFP^+ cell bodies (white arrowheads in A- C). Soma containing
439 vnd^+ positive nuclei that do not seem to be surrounded by GFP in A-C, can be visualized by
440 increased green laser intensity A'- C' (yellow arrowheads), which saturates somas visualized in A-
441 C. Scale bars are 50 μm. n $\geq$ 5 brains. Full genotype: *vnd-T2A-GAL4 w**; 2 x *UAS-mGFP*/+.
442
443 **S5 Fig. *vnd* null mutant clones**
444 (A-B) A representative neuroblast MARCM clone in a wild-type (WT) brain (A) and in a vnd^A brain
445 (B). Scale bar = 50 μm. (C) Number of clones obtained in WT, vnd^A , vnd^6 and $vnd^{\Delta 38}$. Full genotypes:
446 (A) *w* tubP-GAL80 hsFLP122 FRT19A/*w^{1118} *sn FRT19A; c739-GAL4 UAS-mCD8-GFP/*+ (also control
447 hsFLP122 in C). (B) *w* tubP-GAL80 hsFLP122 FRT19A/y* vnd^A *w FRT19A; c739-GAL4 UAS-mCD8-*
448 *GFP/*+ (also vnd^A in C). (C) control hsFLP1: *w tubP-GAL80 hsFLP1 FRT19A* (from the Bloomington
449 stock 5133)/*w UAS-mCD8-GFP sn FRT19A*; *c739-GAL4 UAS-mCD8-GFP/*+. vnd^6: *w tubP-GAL80*
450 *hsFLP1 FRT19A/y* vnd^6 *w UAS-mCD8-GFP sn FRT19A*; *c739-GAL4 UAS-mCD8-GFP/*+. $vnd^{\Delta 38}$: *w*
451 *tubP-GAL80 hsFLP1 FRT19A/*$vnd^{\Delta 38}$ *w UAS-mCD8-GFP FRT19A*; *c739-GAL4 UAS-mCD8-GFP/*+.
452
453
454 ## Acknowledgments
455
456 We thank Aymeric Chartier (IGH, Montpellier) for fruitful discussions regarding the generation of
457 the *Appl* CRISPR alleles. We thank the Bloomington *Drosophila* Stock Center (Indiana University),
458 the BioCampus RAM-*Drosophila* facility and the BioCampus imaging facility MRI (Montpellier,
459 France). We acknowledge BestGene and Genewiz for transgene service and DNA sequencing
460 respectively. The 1D4 anti-Fasciclin II hybridoma and the 8D12 anti-Repo monoclonal antibody
461 developed by Corey Goodman were obtained from the Developmental Studies Hybridoma Bank,
462 created by the NICHD of the NIH and maintained at the University of Iowa, Department of Biology,
463 Iowa City, IA 52242. We thank Chris Doe for the $vnd^{\Delta 38}$ and vnd^6 alleles and Tzumin Lee for the
464 *vnd-T2A-GAL4* line.
465
466 **Funding:** C.M. was supported by a PhD grant from the Ministère de l'Enseignement Supérieur et
467 de la Recherche. C.M. and G.U.B. were supported by the Fondation pour la Recherche Médicale
468 (FRM) respectively for the 4th PhD year and for a 3-year post-doctoral fellowship. Work in the
469 laboratory of J.-M.D. was supported by the Centre National de la Recherche Scientifique (CNRS),
470 the Association pour la Recherche sur le Cancer (grants PJA 20151203422), the FRM (Programme
471 "EQUIPES FRM2016" project DEQ20160334870) and the ANR 2021 ORIO.
472
473
474 ## References
475 **Aso, Y., Grubel, K., Busch, S., Friedrich, A. B., Siwanowicz, I. and Tanimoto, H.** (2009). The
476 mushroom body of adult Drosophila characterized by GAL4 drivers. *J Neurogenet* **23**, 156–
477 172.

478 **Boulanger, A., Clouet-Redt, C., Farge, M., Flandre, A., Guignard, T., Fernando, C., Juge, F. and**
479 **Dura, J. M.** (2011). ftz-f1 and Hr39 opposing roles on EcR expression during Drosophila
480 mushroom body neuron remodeling. *Nat Neurosci* **14**, 37–44.
481 **Cassar, M. and Kretzschmar, D.** (2016). Analysis of Amyloid Precursor Protein Function in
482 Drosophila melanogaster. *Front Mol Neurosci* **9**, 61.
483 **Chen, H. M., Huang, Y., Pfeiffer, B. D., Yao, X. and Lee, T.** (2015). An enhanced gene targeting
484 toolkit for Drosophila: Golic+. *Genetics* **199**, 683–694.
485 **Chu, H., Parras, C., White, K. and Jimenez, F.** (1998). Formation and specification of ventral
486 neuroblasts is controlled by vnd in Drosophila neurogenesis. *Genes Dev* **12**, 3613–3624.
487 **Doudna, J. A. and Charpentier, E.** (2014). Genome editing. The new frontier of genome
488 engineering with CRISPR-Cas9. *Science* **346**, 1258096.
489 **Haelterman, N. A., Jiang, L., Li, Y., Bayat, V., Sandoval, H., Ugur, B., Tan, K. L., Zhang, K., Bei, D.,**
490 **Xiong, B., et al.** (2014). Large-scale identification of chemically induced mutations in
491 Drosophila melanogaster. *Genome Res* **24**, 1707–1718.
492 **Jimenez, F., Martin-Morris, L. E., Velasco, L., Chu, H., Sierra, J., Rosen, D. R. and White, K.** (1995).
493 vnd, a gene required for early neurogenesis of Drosophila, encodes a homeodomain
494 protein. *EMBO J* **14**, 3487–3495.
495 **Lee, T., Lee, A. and Luo, L.** (1999). Development of the Drosophila mushroom bodies: sequential
496 generation of three distinct types of neurons from a neuroblast. *Development* **126**, 4065–
497 4076.
498 **Lee, T. and Luo, L.** (1999). Mosaic analysis with a repressible cell marker for studies of gene
499 function in neuronal morphogenesis. *Neuron* **22**, 451–461.
500 **Lee, Y. J., Yang, C. P., Miyares, R. L., Huang, Y. F., He, Y., Ren, Q., Chen, H. M., Kawase, T., Ito,**
501 **M., Otsuna, H., et al.** (2020). Conservation and divergence of related neuronal lineages in
502 the Drosophila central brain. *Elife* **9**.
503 **Leyssen, M., Ayaz, D., Hebert, S. S., Reeve, S., De Strooper, B. and Hassan, B. A.** (2005). Amyloid
504 precursor protein promotes post-developmental neurite arborization in the Drosophila
505 brain. *EMBO J* **24**, 2944–2955.
506 **Lin, S.** (2023). The making of the Drosophila mushroom body. *Front Physiol* **14**, 1091248.
507 **Liu, T., Zhang, T., Nicolas, M., Boussicault, L., Rice, H., Soldano, A., Claeys, A., Petrova, I., Fradkin,**
508 **L., De Strooper, B., et al.** (2021). The amyloid precursor protein is a conserved Wnt
509 receptor. *Elife* **10**.
510 **Luo, L., Tully, T. and White, K.** (1992). Human amyloid precursor protein ameliorates behavioral
511 deficit of flies deleted for Appl gene. *Neuron* **9**, 595–605.
512 **Marquilly, C., Busto, G. U., Leger, B. S., Boulanger, A., Giniger, E., Walker, J. A., Fradkin, L. G.**
513 **and Dura, J. M.** (2021). Htt is a repressor of Abl activity required for APP-induced axonal
514 growth. *PLoS Genet* **17**, e1009287.
515 **Nicolas, M. and Hassan, B. A.** (2014). Amyloid precursor protein and neural development.
516 *Development* **141**, 2543–2548.
517 **Port, F., Chen, H. M., Lee, T. and Bullock, S. L.** (2014). Optimized CRISPR/Cas tools for efficient
518 germline and somatic genome engineering in Drosophila. *Proc Natl Acad Sci U S A* **111**,
519 E2967–2976.

520 **Rabah, Y., Berwick, J. P., Sagar, N., Pasquer, L., Placais, P. Y. and Preat, T.** (2025). Astrocyte-to-
521 neuron H(2)O(2) signalling supports long-term memory formation in Drosophila and is
522 impaired in an Alzheimer's disease model. *Nat Metab* **7**, 321–335.
523 **Selkoe, D. J. and Hardy, J.** (2016). The amyloid hypothesis of Alzheimer's disease at 25 years.
524 *EMBO Mol Med* **8**, 595–608.
525 **Soldano, A. and Hassan, B. A.** (2014). Beyond pathology: APP, brain development and Alzheimer's
526 disease. *Curr Opin Neurobiol* **27**, 61–67.
527 **Soldano, A., Okray, Z., Janovska, P., Tmejova, K., Reynaud, E., Claeys, A., Yan, J., Atak, Z. K., De**
528 **Strooper, B., Dura, J. M., et al.** (2013). The Drosophila Homologue of the Amyloid
529 Precursor Protein Is a Conserved Modulator of Wnt PCP Signaling. *PLoS biology* **11**,
530 e1001562.
531 **Stepchenko, A. G., Pankratova, E. V., Doronin, S. A., Gulag, P. V. and Georgieva, S. G.** (2011). The
532 alternative protein isoform NK2B, encoded by the vnd/NK-2 proneural gene, directly
533 activates transcription and is expressed following the start of cells differentiation. *Nucleic*
534 *Acids Res* **39**, 5401–5411.
535

Figure 1

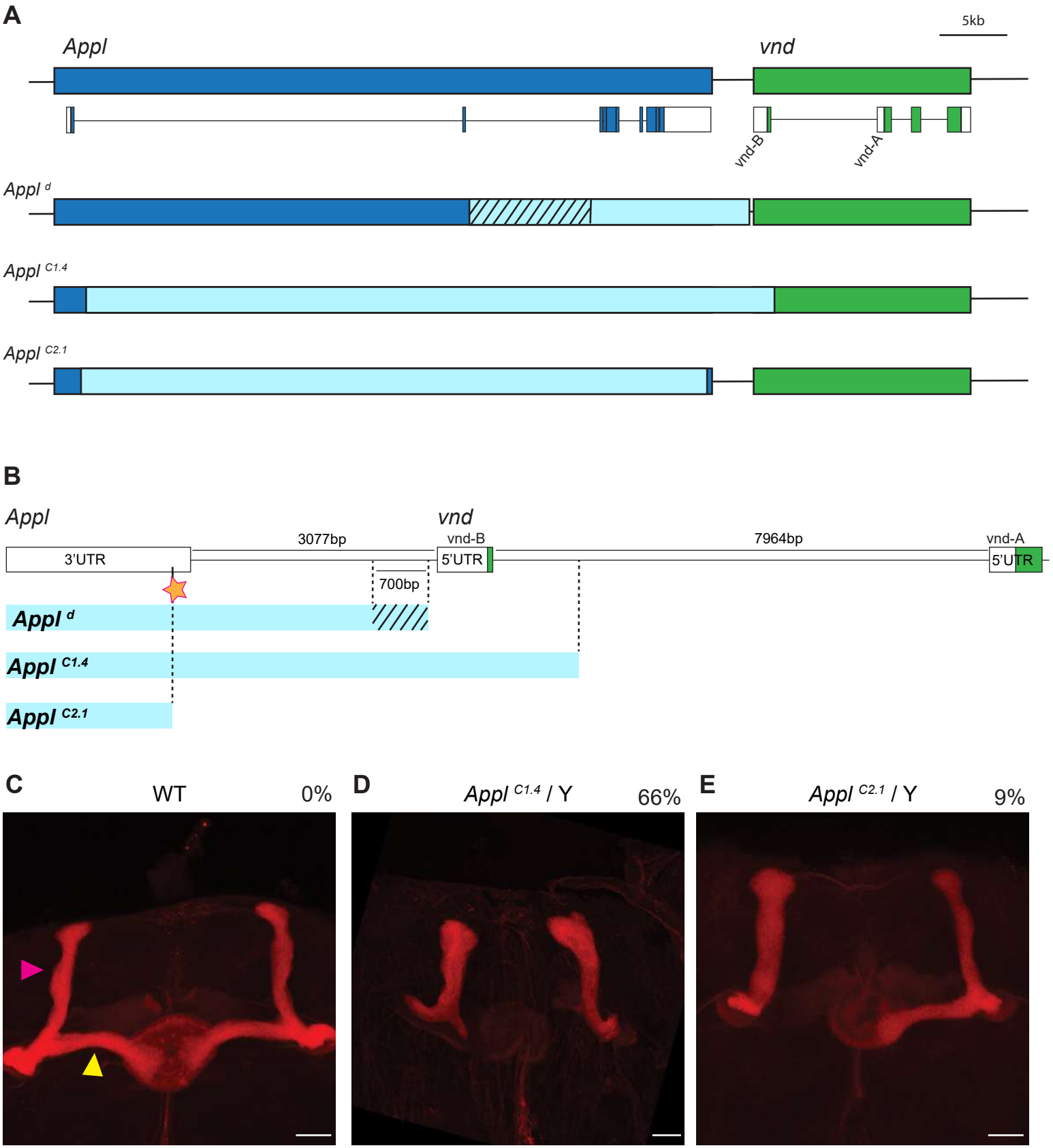
A
5kb
Appl
vnd
vnd-B
vnd-A
Appl d
Appl C1.4
Appl C2.1
B
Appl
vnd
3077bp
vnd-B
7964bp
vnd-A
3'UTR
5'UTR
5'UTR
700bp
Appl d
Appl C1.4
Appl C2.1
C
WT
0%
D
Appl C1.4 / Y
66%
E
Appl C2.1 / Y
9%

Figure 2

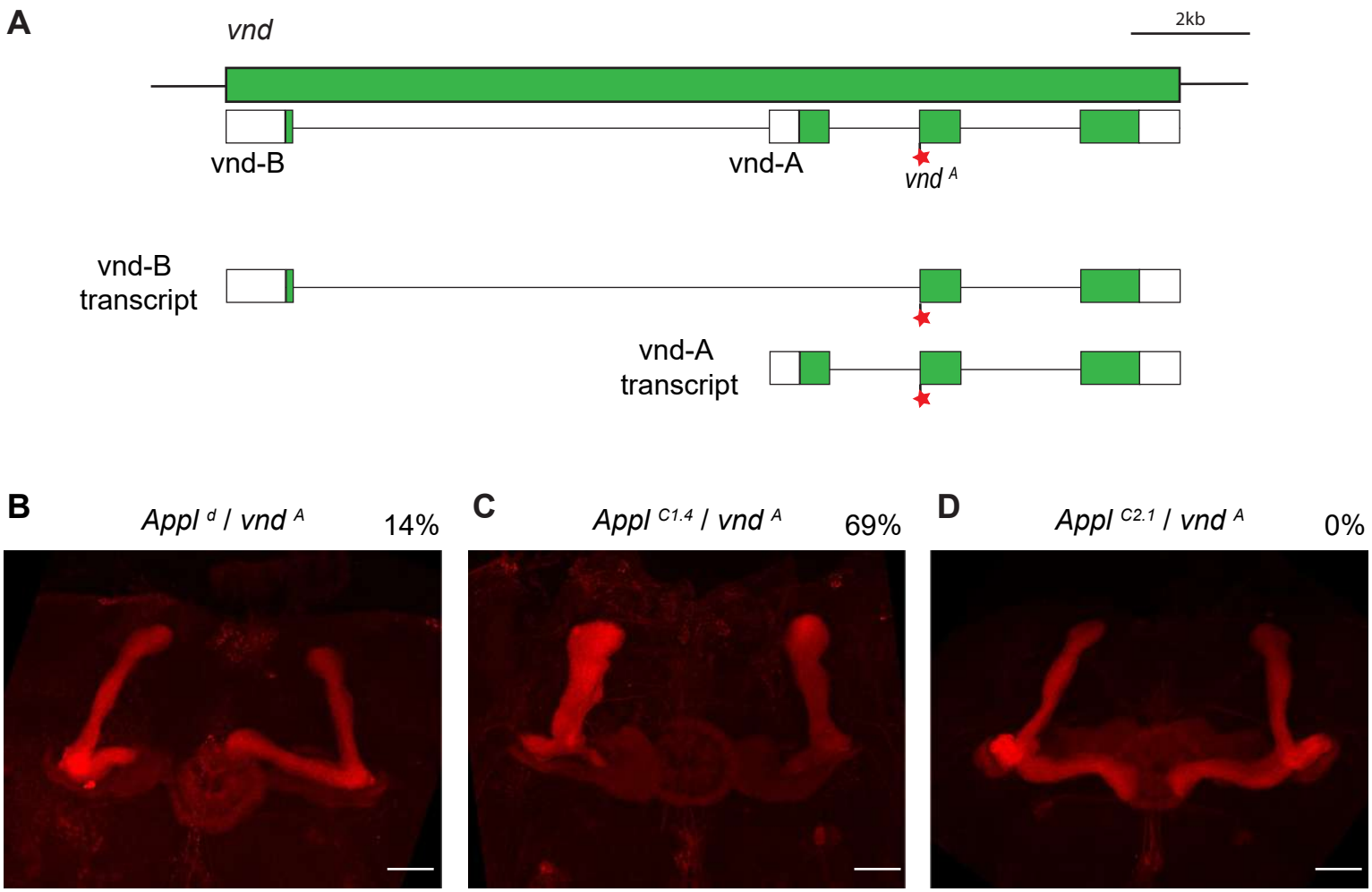
A
vnd
2kb
vnd-B
vnd-A
vnd A
vnd-B transcript
vnd-A transcript
B
Appl d / vnd A
14%
C
Appl C1.4 / vnd A
69%
D
Appl C2.1 / vnd A
0%

Figure 3

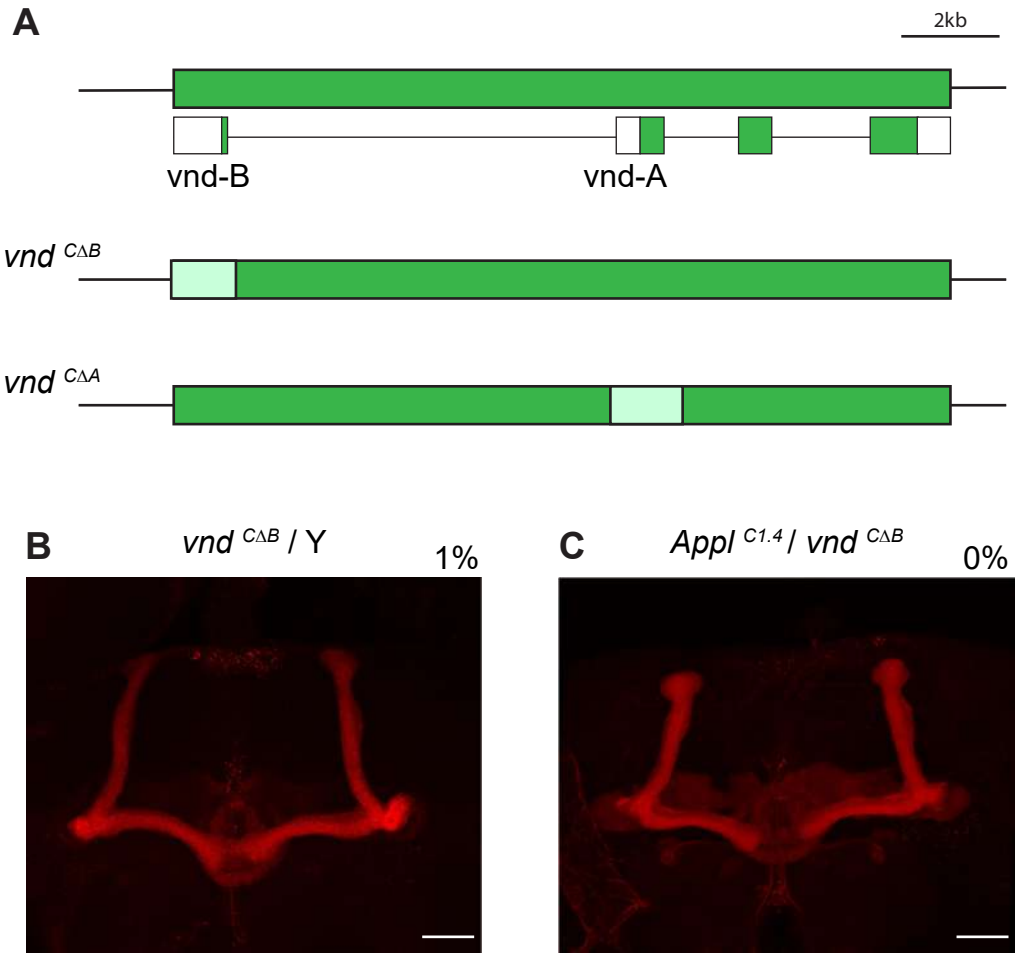

Figure 4

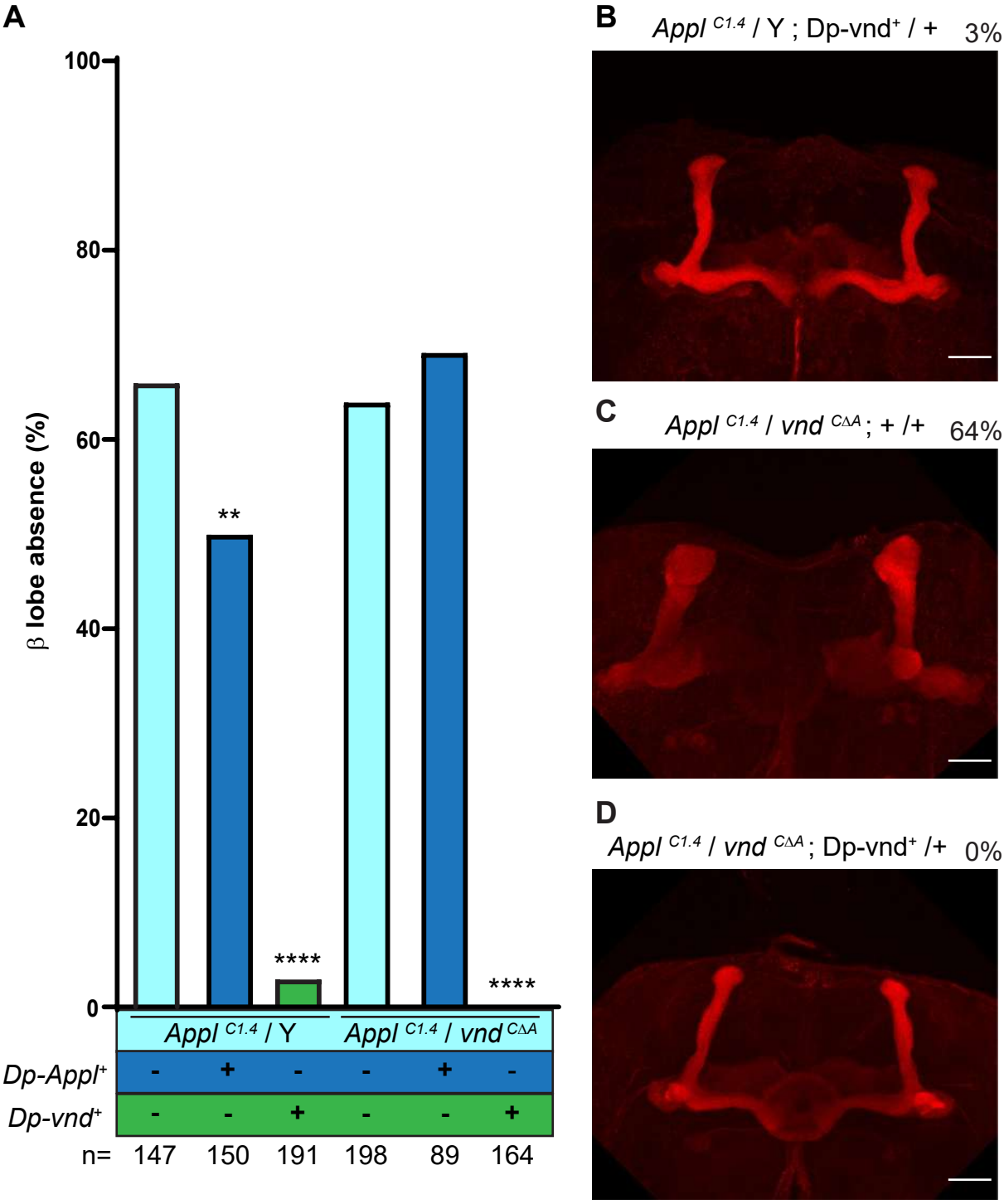
A
100
80
60
40
20
0
β lobe absence (%)
**
****
****
Appl C1.4 / Y
Appl C1.4 / vnd CΔA
Dp-Appl+
Dp-vnd+
n= 147 150 191 198 89 164
B
Appl C1.4 / Y ; Dp-vnd+ / + 3%
C
Appl C1.4 / vnd CΔA ; + /+ 64%
D
Appl C1.4 / vnd CΔA ; Dp-vnd+ /+ 0%

Figure 5

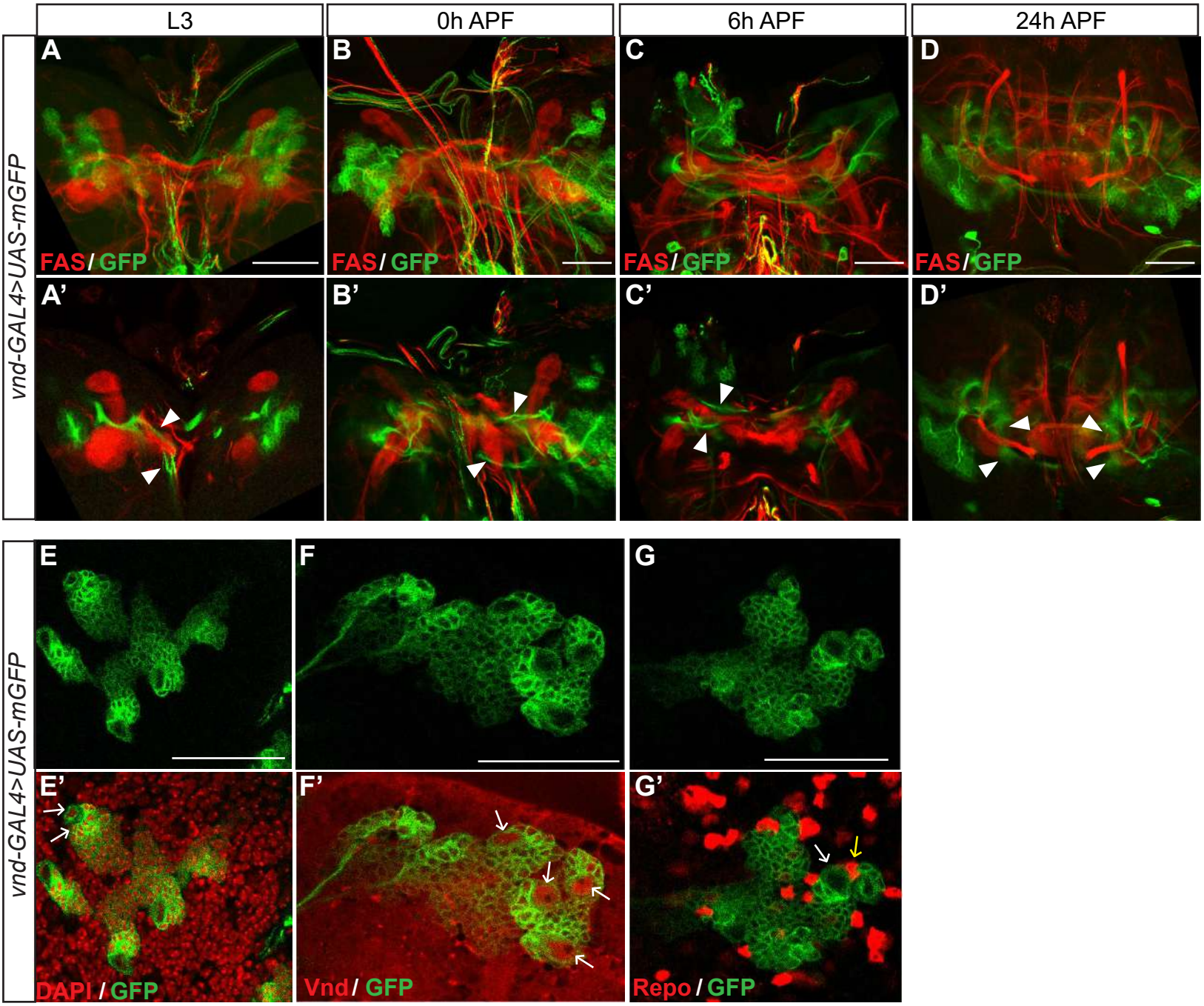
L3
0h APF
6h APF
24h APF
vnd-GAL4>UAS-mGFP
A
B
C
D
FAS / GFP
A'
B'
C'
D'
E
F
G
E'
F'
G'
DAPI / GFP
Vnd / GFP
Repo / GFP

Figure S1 - related to Figure 1

A

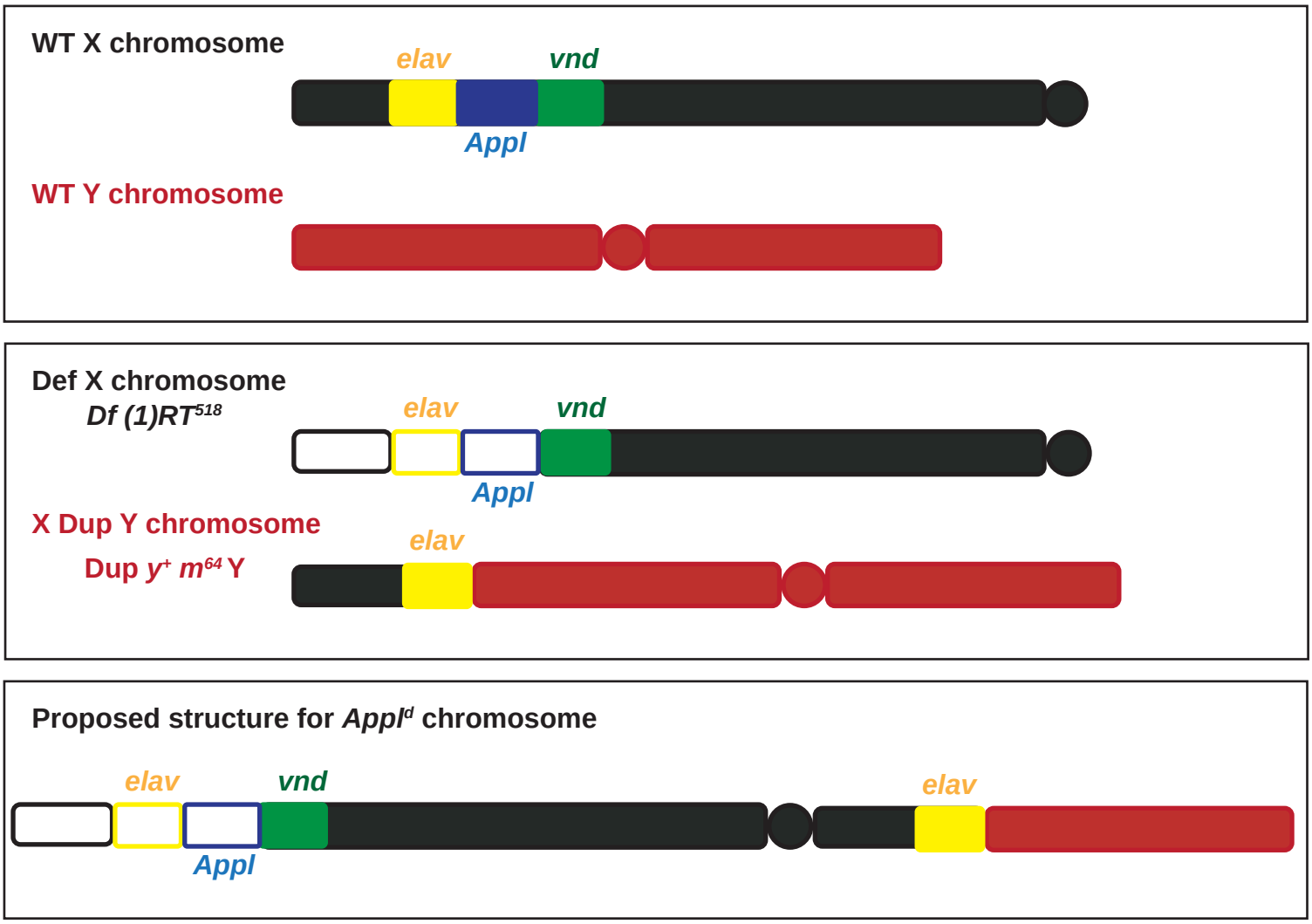

Figure S2 - related to Figure 1

A

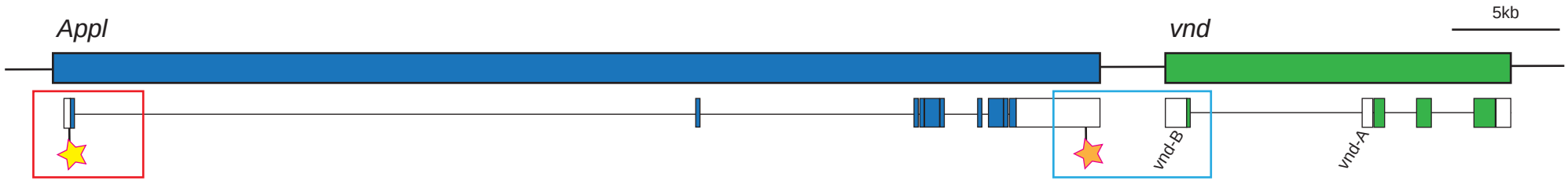

B

Appl 5'- CCGTCGTCCGCCTGTGCAGCAAAGTGTTAAACGAAT -- 971bp -- GATTGGGGATGGGTATGG - 3'

Appl $^{C1.4}$ 5' - CCGTCGTCCGCCTGTGCAGCAAAGTGTTAAACGAAT -- 971bp -- GATTGG - 3'

C

Appl 5'- ATTCTGTCCTGGCGACTAAGCCCCGATATTTGAT -- 5958bp -- TATGAAGTTCGAAAAAATAATTTCATTTTAACG - 3' ***vnd***

Appl $^{C1.4}$ 5' - AAAAAATAATTTCATTTTAACG - 3'

D

Appl 5'- CTGCTACCGTCGTCCGCCTGTGCAGCAAAGTGTTAAACGAATAG --- 47056 bp --- AGCATTCTGTCCTGGCGACTAAGCCCCGATATTTGATCTTCGATCG - 3'

Appl $^{C2.1}$ 5'- CTGCTACCGTCGTCCGCCT ACTAAGCCCCGATATTTGATCTTCGATCG - 3'

Insertion of 821 bp

Figure S3 - related to Figure 3

A

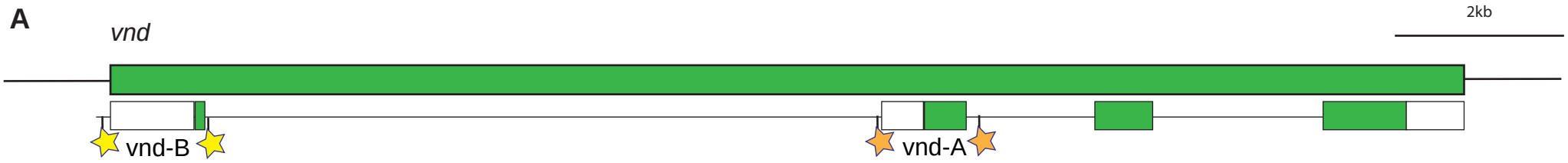

B

vnd

5’- GGGGGCAGCGATAACTGCAGCTCACACCTACAGGGATAGCTTTATCGA -1069bp- TTCTGAACCCAAAATCACGAATCAAAAATGAGCCGACGGCGAATGGGCACAG - 3’

5’ - GGGGGCAGCGATAACTGCAGCTC CGGCGAATGGGCACAG - 3’

vnd $^{C\Delta B}$

C

vnd

5’- GATACCCAAAGACACCCCGAGCATACGACCTGGTACTTTTCTGCCGTT --1608bp-- TTTAAATTAACCAAGCGGGCACAGCGCGCAAGTACAGGACAGGGTATAAT - 3’

5’ - GATACCCAAAGACA GGACAGGGTATAAT - 3’

vnd $^{C\Delta A}$

Figure S4 - related to Figure 5

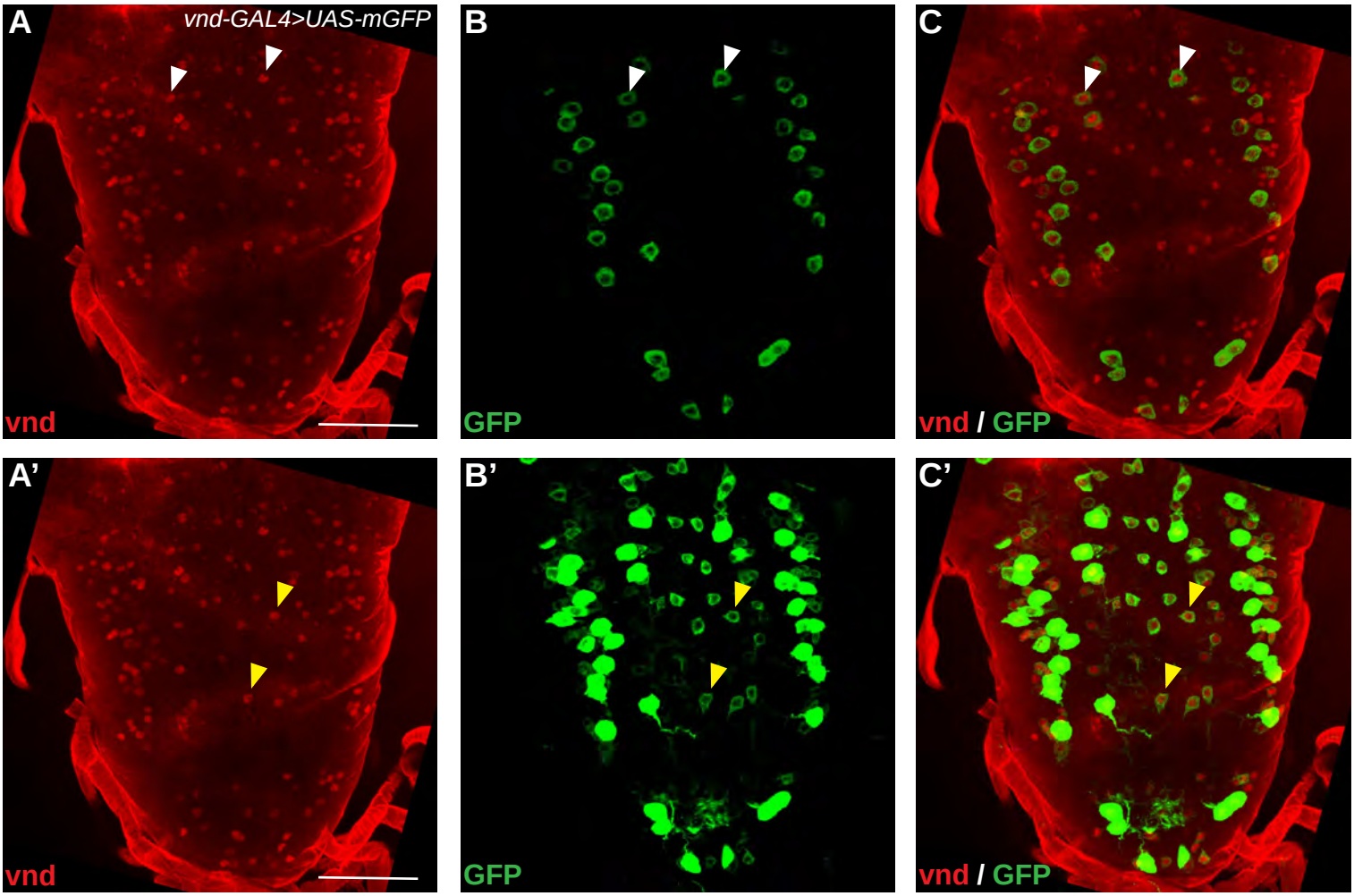

Figure S5 - related to Figure 4

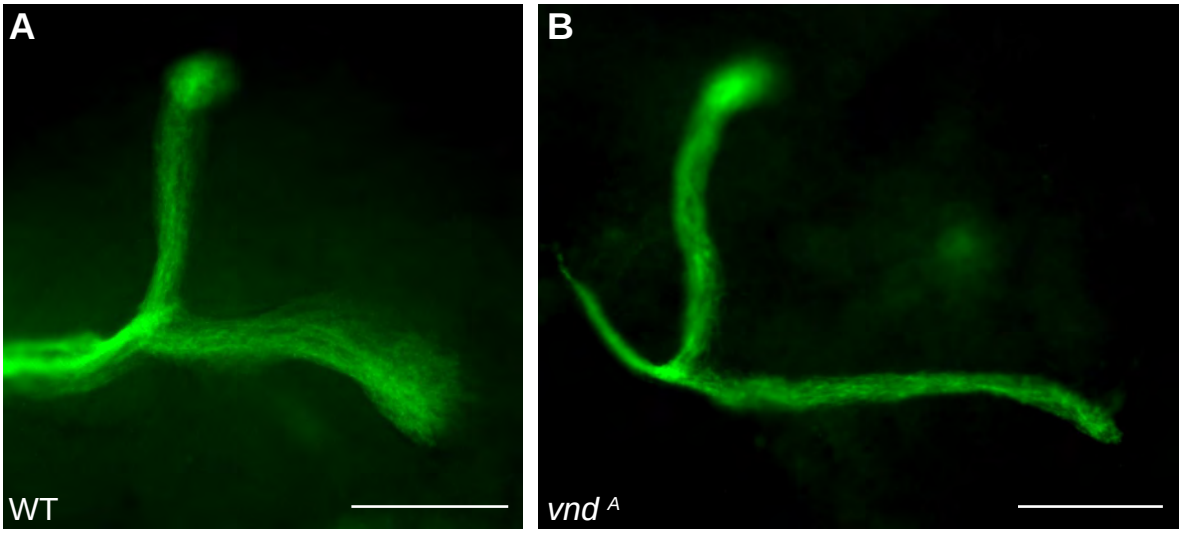

C

Clone Genotypes	MB observed	MB clones		WT looking clones	
control hsFLP122	126	36	29%	36	100%
vnd ^{A}	76	20	26%	20	100%
control hsFLP1	56	5	9%	5	100%
vnd ^{6}	34	4	12%	4	100%
vnd $^{\Delta 38}$	90	8	9%	8	100%